

Influence of process parameters on carbonation rate and conversion of steelmaking slags – Introduction of the ‘carbonation weathering rate’

Evangelos Georgakopoulos¹, Rafael M. Santos^{2,*}, Yi Wai Chiang³, Vasilije Manovic^{1,*}

¹ Cranfield University, School of Engineering, Cranfield, MK43 0AL, United Kingdom.

² Sheridan Institute of Technology, School of Applied Chemical and Environmental Sciences, Chemical and Environmental Laboratories (CEL), Brampton, Ontario, Canada, L6Y 5H9.

³ University of Guelph, School of Engineering, Guelph, Ontario, Canada, N1G 2W1.

* Corresponding authors: rafael.santos@alumni.utoronto.ca (RMS); v.manovic@cranfield.ac.uk (VM).

Abstract

Alkaline industrial wastes are considered as potential resources for the mitigation of CO₂ emissions by simultaneously capturing and sequestering CO₂ through mineralization. Mineralization safely and permanently stores CO₂ through its reaction with alkaline earth metals. These elements are found in a variety of abundantly available industrial wastes that have high reactivity with CO₂, and that are generated close to the emission point-sources. Among all suitable industrial wastes, steelmaking slag has been deemed the most promising given its high CO₂ uptake potential. In this article, we review recent publications related to the influence of process parameters on the carbonation rate and conversion extent of steelmaking slags, comparing and analyzing them in order to define the present state of the art. Furthermore, the maximum conversions resulting from different studies are directly compared using a new index, the Carbonation Weathering Rate (CWR), which normalizes the results based on particle size and reaction duration. To date, the carbonation of Basic Oxygen

Furnace steelmaking slag, under mild conditions, presents both the highest carbonation conversion and CWR, with values equal to 93.5% and 0.62 $\mu\text{m}/\text{min}$, respectively.

Keywords

CO₂ mineralization; Industrial wastes; Steelmaking slags; Carbonation conversion;

Weathering rate

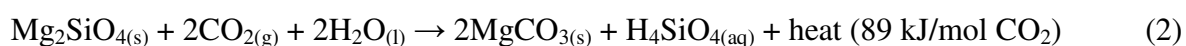
1. INTRODUCTION

Since measurements of atmospheric CO₂ began in Mauna Loa (Hawaii), on March 1958, the annual mean concentration has increased from 315.97 ± 0.12 ppmv to a markedly historical value of 400.83 ± 0.12 ppmv (in 2015);¹ this is an elevation of about 27% over the last six decades. In the same timeframe, the global land and ocean surface temperature anomaly (defined with respect to the period 1901-2000) has increased by exactly 1°C, from an annual average of 0.11°C to 1.11°C.² This correlation, and extensive climate studies, strongly suggests a link between CO₂ emissions and global warming. In fact, it has been suggested, by climate modeling, that if the anthropogenic CO₂ emissions continue to follow the current trends, the mean surface temperature of the Earth will be raised by 2.1–4.6 °C, if the CO₂ concentration doubles from pre-industrial levels.³

Following these serious threats, at the Paris climate conference (COP21), in December 2015, 195 countries adopted the first-ever universal, legally binding global climate deal (to come into force in 2020), which sets out a global action plan to limit global warming to “well below 2°C”, and preferably below 1.5°C.⁴ To mitigate the anthropogenic CO₂ emissions, several solutions have been proposed. Among solutions that include the improvement of fuel conversion efficiency and the usage of renewable fuels, carbon capture and storage (CCS) is considered an essential technology in the global effort to mitigate climate change,⁵ and it is a solution that could allow continued use of fossil fuels while reducing greenhouse gas (GHG)

emissions.⁶ CCS technology, though largely still under demonstration (e.g., IEAGHG Weyburn-Midale CO₂ Monitoring and Storage Project, concluded in 2012, has stored 22 Mt of CO₂),⁷ is still regarded as a promising technology for climate change mitigation.

Among the various CCS mechanisms, mineral trapping is attractive as it manages to store CO₂ by transforming it into a solid carbonate mineral, which can remain stable over geological timeframes.⁸ This process can occur either naturally, under ambient conditions, or in laboratory/industrial settings, under controlled conditions. Naturally occurring CO₂ mineralization is known as “silicate weathering”.⁹ CO₂ reacts exothermically with alkaline earth metals-bearing silicates, forming thermodynamically stable and environmentally benign carbonates. Typical reactions are exemplified by:¹⁰



The main drawback of the natural weathering process in terms of mineralization is the very slow kinetics, mainly due to the very low concentration of CO₂ in rainwater (approximately 1–2 mg/L).¹¹ In the last two decades, many researchers have been working on accelerating the reactions between CO₂ and alkaline minerals. Seifritz¹² was one of the first to propose the accelerated carbonation process in which carbon dioxide of high pressure and high purity reacts with alkaline materials in the presence of moisture, in order to accelerate the reaction to a timescale of a few minutes or hours. The exothermic nature of the occurring reactions is a remarkable characteristic of the process (Eqns (1)–(3)). Since a significant amount of energy is required as an input for industrial accelerated carbonation (due to required milling, pumping, compression, heating, sorbent regeneration, etc.), the heat released by the reaction

could be recovered and used to compensate the energy input.¹³ As a result, the costs of the process could be lowered.¹⁴

Accelerated carbonation can be classified into two processes: the direct carbonation, where carbonation takes place in a single step (in one reactor), and the indirect carbonation, where the alkaline earth metals are first extracted from the mineral matrix in one reactor and subsequently carbonated in another reactor.¹⁵ Direct carbonation can occur by following two procedures: i) under the gas–solid direct dry carbonation, operated at liquid-to-solid (L/S) ratio of less than 0.2 L/kg, the alkaline earth metals present in silicate minerals are converted directly to carbonates using gaseous or supercritical CO₂, and ii) under the aqueous (wet/slurry) carbonation, operated at L/S ratio of more than 0.2 L/kg, the alkaline earth metals are extracted from the silicate mineral, using acids such as acetic acid,¹⁵ and subsequently carbonated.¹⁶

The most commonly used natural silicates containing alkaline earth metal oxides for carbonation are olivine (Mg₂SiO₄), serpentine (Mg₃Si₂O₅(OH)₄) and wollastonite (CaSiO₃).¹⁷

An alternative to natural minerals, which require energy-intensive mining and mineral processing for utilization, are industrial residues. Several waste materials are qualified as efficient reactants for CO₂ mineralization due to their high alkaline earth metal content, as well as their proximity to CO₂ emission point sources. The most common industrial residues suitable for this process are: bottom ash and fly ash from municipal solid waste incineration processes, pulverized fuel ash produced by coal-fired power plants, iron-making slag, carbon steel-making slag, stainless steel-making slags, mining tailings, red mud, asbestos-containing residues, and oil-shale processing residues.¹⁸ Due to the variable nature of these materials (different composition, mineralogy, morphology), each requires a different processing technology, the CO₂ uptake amounts are highly variable, and the fate of the resulting

carbonates can be a disposal site (e.g., mine backfill)¹⁹ or in a commercial application (e.g., building materials).²⁰

The amount of available alkaline earth metals contained in these residues, worldwide, is capable of storing a limited amount of CO₂ annually. Kirchofer et al.²¹ estimate that in the USA, industrial alkaline byproducts have the potential to mitigate approximately 7.6 Mt CO₂/a (7.0 Mt/a by mineralization and 0.6 Mt/a by avoided emissions). If this amount is extrapolated worldwide in proportion to the industrial fraction of the nominal gross domestic product (GDP) of each country (\$3.33T (19.1% of 2014 GDP) for the U.S., \$22.8T (30.5% of 2014 GDP) for the world)²², potentially 52.0 Mt CO₂/a could be mineralized using industrial residues. This represents a small fraction of CO₂ emissions worldwide, which are nearing 40 Gt CO₂/a.²³ Although their contribution to the mitigation of GHGs is small, attention should be paid to the carbonation of these types of materials for the following reasons:

- This process can substantially reduce the CO₂ emissions of specific industrial sectors, where integration with mineral carbonation can be rather efficiently achieved, such as iron- and steel-making or cement manufacturing industries.
- It is a way to make the disposal (landfilling) of such residues less hazardous, in an economical way.^{18,24}
- This technology also produces carbonates that can be used commercially in several applications, for instance, as synthetic aggregates with more favorable characteristics regarding their implementation in construction applications, than the untreated raw material.^{20,25}

Slags are generated during the steel production process, and these amount to approximately 10 - 15 wt% of the steel produced.²⁶ The slags are classified based on the steel-making process; i.e., blast furnace (BF) slags from the iron-making process, basic oxygen furnace (BOF) slags or electric arc furnace (EAF) slags from the steel-making process, and argon-

oxygen decarburization (AOD) slags and continuous casting (CC) slags from the refining process. These residues have low commercial value due to their composition: little metallic iron and large amounts of mixed oxides such as CaO, SiO, MgO, Al₂O₃ and MnO.²⁷ They also contain detectable amounts of toxic components such as As, Cd, Cr, Hg, Pb and Se,²⁸ which is concerning for their reuse.

The large generation rate of slags, the limited commercial market, rising landfill fees and tightening environmental regulations are a growing concern for the industry. In 2015, the worldwide blast furnace slag production was approximately 300-360 Mt based on typical ratios of slag to crude iron output.²⁹ Carbonation of iron- and steel-making slags could be an efficient technology to store a significant percentage of CO₂ emitted from steel-making plants, while at the same time reducing their toxicity and generating new revenue streams. Opportunely, iron- and steel-making slags also present the highest experimental CO₂ uptake (ECO₂) compared with other industrial wastes. It has been reported that BF slag presents an ECO₂ uptake of 75–294 g CO₂/kg slag;^{30,31} BOF slag attributes an ECO₂ uptake of approximately 266 g/kg;³²⁻³⁴ EAF slag has demonstrated an ECO₂ uptake of 136–220 g/kg;^{35,36} AOD slag has presented ECO₂ uptakes of between 190–429 g/kg;^{37,38} and CC slag has realized an ECO₂ uptake of 312 g CO₂/kg slag.³⁹

In this review, the effects of different parameters on the carbonation extent and kinetics of different types of iron- and steel-making slags under various experimental conditions are discussed, compared and analyzed. Furthermore, a new index, the Carbonation Weathering Rate (CWR), is introduced to facilitate comparison among results obtained from different studies, as different particle sizes are used, and particle size considerably affects carbonation rate and conversion. The CWR is the growth rate of the thickness of the reacted layer of a carbonated particle, and takes the initial particles size distribution into consideration to account for complete and partial conversion depending on particle size.

2. IRON- AND STEEL-MAKING SLAG CARBONATION: A LITERATURE REVIEW OF CONVERSION EXTENT AND KINETICS

In this section, literature on the carbonation of iron- and steel-making slags is reviewed. All relevant results from the cited studies are summarized in Tables 1 and 2 to facilitate comparison. These results are discussed in the following subsections.

2.1 Blast furnace (BF) slag

Blast furnace slag is generated during the iron-making stage of the steel manufacturing process. The aqueous slurry carbonation kinetics of this type of slag were tested by Chang et al.⁴⁰ using an autoclave reactor and slag particles of less than 44 μm . Four different parameters were studied regarding their effect on the carbonation extent of the slag: reaction time, temperature, CO_2 partial pressure, and liquid-to-solid (L/S) ratio.

Reaction time: Chang et al.⁴⁰ found that, up to 60 minutes of reaction duration, the carbonation extent increases, and that after this point it levels off. Furthermore, it is also noted that the carbonation rate decreases with time within the first 60 minutes.

Temperature and CO_2 pressure: at a pressure of 48.3 bar, the increase of temperature up to 100 °C leads to an increase of the conversion extent. Further temperature increase over 100 °C causes a decrease in the conversion extent. This behavior is not observed when the partial pressure of CO_2 is 89.6 bar (supercritical condition). In this case, the conversion extent continues to increase even after 100 °C. This was explained by Chang et al.⁴⁰ by the fact that, with increasing temperature, Ca^{2+} leaching increases, whereas CO_2 dissolution decreases. Up to 100 °C, Ca^{2+} leaching overcame the attenuation of CO_2 dissolution, leading to an increase of conversion. For temperatures over 100 °C, the reduced CO_2 dissolution becomes the limiting factor of the carbonation reaction, and the conversion decreases accordingly.

However, when the CO₂ partial pressure was maintained at 89.6 bar, the higher CO₂ solubility and lower dynamic viscosity permitted the Ca²⁺ leaching to be the limiting factor of the carbonation reaction, even at elevated temperatures over 100 °C.

Liquid-to-solid ratio: Chang et al.⁴⁰ reported the optimal L/S ratio to be 10 L/kg. For L/S ratio equal to zero (i.e., dry solids), the conversion extent was very low due to the absence of water. For L/S values below optimal, the slurry did not mix well in the reactor, resulting in poor contact between the solid particles and the reaction fluid. For L/S ratio above the optimal, a mass transfer barrier was created due to the excessive presence of water, and the ionic strength decreased, slowing leaching and the mixing of CO₂ with Ca²⁺ ions.

2.2 Basic oxygen furnace (BOF) slag

Basic oxygen furnace slag is generated during the steel-making stage of the steel manufacturing process. The carbonation kinetics of this type of slag were studied by Huijgen et al.⁴¹ using a continuously-stirred autoclave reactor, by Chang et al.⁴²⁻⁴⁴ using several types of reactors (column slurry reactor,^{42,43} and high-gravity rotating packed bed⁴⁴), by van Zomeren et al.⁴⁵ using column reactors, by Polettini et al.⁴⁶ and Baciocchi et al.⁴⁷ using a stirring pressurized stainless steel reactor, and by Tai et al.³³ using a continuously-stirred high-pressure batch reactor. The direct dry carbonation of BOF slag was tested by Santos et al.⁴⁸, who performed the carbonation experiments using different experimental set-ups (thermogravimetric reactor, pressurized basket reactor, atmospheric furnace). The effects of temperature, reaction time, CO₂ pressure, L/S ratio and particle size on carbonation conversion and kinetics were investigated in the aforementioned.

Temperature: up to the optimal temperature, which was different in each study, the conversion extent and rate increased with the temperature increase. During this regime, Ca²⁺ dissolution and diffusion was the limiting factor of the carbonation conversion, with

increasing temperature contributing to faster and more complete dissolution. However, further increase of temperature resulted in a decrease in both the carbonation extent and rate. In this regime, the CO₂ solubility becomes the limiting factor of the carbonation; lower solubility slowed the reaction rate and ultimately the conversion extent. It also appears that at elevated temperatures two phases of carbonation occurred. During the first phase of carbonation, much of the available calcium dissolved rapidly into the solution, leading to high initial conversion rate. Later on, the reaction considerably slowed as the remaining calcium was slow to dissolve and react. As a result, conversion was not maintained at the same rate throughout the process.

There are also occasions where temperature does not have any particular effect on the conversion extent or rate, such as reported by van Zomeren et al.,⁴⁵ where under unsaturated conditions (L/S ratio = 0.01-0.1 L/kg), the increase in temperature was not reported as having an impact on the carbonation of the tested BOF slag. This, however, can be due to the temperature range (5-90 °C in this case) not surpassing the point at which enhanced dissolution stops making up for lower CO₂ solubility.

Several studies apply reaction temperatures that are below the optimum (i.e., reaction rate and conversion are still improving at the maximum temperature tested). Researchers do this in part to save energy demand of the process, which is important from the point of view of maximizing net CO₂ sequestration. As such, the negative impact of increasing temperature is not reported in these works. One example of this is the recent study of Polettini et al.⁴⁶, where temperature increase (up to 100 °C) led to continuous carbonation enhancement. Huijgen et al.⁴¹, using a similar experimental process, reported the optimum temperature for the carbonation of such slags lying at approximately 175 °C.

Reaction time: the effect of reaction time on carbonation rate was similar for every case studied. Initially, the carbonation extent increased as the rate decreased, and levelled off

afterwards. The length of this initial period was different in each study, ranging from 5 min⁴⁴ to 24 h⁴⁵, and it was mainly dependent on the experimental process and the other parameters of the carbonation (temperature, CO₂ pressure, etc.). The main reason for this effect is the pore blockage of the slag particles due to the precipitation of the newly formed CaCO₃. The newly formed calcite creates a barrier that inhibits the diffusion of the Ca²⁺ ions from the solid slag particle to the solution.⁴⁹ In some cases, mineralogy also limits the ultimate reaction extent.³⁹

Particle size: one of the most significant parameters that determines the carbonation extent is the particle size. Huijgen et al.⁴¹ and Santos et al.⁴⁸ investigated the influence of BOF slag particle size on the carbonation extent. It was observed that the reduction of the particle size resulted in the increase in the specific surface area of the slag, and a significant increase in the carbonation conversion. Huijgen et al.⁴¹ studied the slurry carbonation of BOF slag and observed that by reducing the particle size from <1 mm to <38 µm, the conversion extent increased from 24% to 74%. Similarly, Santos et al.⁴⁸ studied the direct carbonation of BOF slag in a pressurized basket reactor and identified a critical dependence of the CO₂ uptake on the particle size. By reducing the particle size from <1.6 mm to <0.08 mm, the free lime conversion extent significantly increased from 8% to 43%.

CO₂ pressure: the influence of CO₂ pressure on the carbonation of BOF slags was tested by Huijgen et al.⁴¹, Santos et al.⁴⁸, and Polettini et al.⁴⁶. Huijgen et al.⁴¹ showed that the effect of CO₂ pressure on the conversion extent and rate achieved by the slurry carbonation of BOF slag was negligible for temperatures below the optimal, CO₂ pressure above 90 bar, and stirring speed more than 500 rpm. This further supports the previous findings that present the Ca²⁺ leaching as the limiting factor of carbonation at such temperatures. For CO₂ pressures and stirring speeds below the aforementioned values, the conversion extent decreased,

respectively, due to limited dissolution of CO₂ into the solution and low quality of mixing between the different phases.

Santos et al.⁴⁸ observed a different influence of CO₂ pressure on the CO₂ uptake achieved by the direct carbonation of BOF slag. The authors found that the effect of increasing CO₂ pressure on the CO₂ uptake was highly dependent on the reaction temperature. At lower temperatures (350 °C) the increase of the CO₂ pressure resulted in a more significant uptake enhancement (+176% at 20 bar over 4 bar), whereas at higher temperatures (500 °C) this improvement in CO₂ uptake was significantly lower (+7% at 20 bar over 4 bar), and no improvement was detectable at 650 °C.

Polettini et al.⁴⁶ examined the influence of CO₂ pressure on the carbonation extent in correlation with the CO₂ concentration in the gas phase. They tested three different CO₂ concentrations (10%, 40% and 100%), and showed that for concentrations of 10% and 40% the effect of CO₂ partial pressure on the conversion was most relevant for pressures up to 6 bar. After this particular value, the CO₂ uptake levelled off. Furthermore, it was found that for pure CO₂, the influence of the CO₂ pressure on the carbonation yield was remarkably lower.

Although CO₂ pressure enhancement should lead to carbonation conversion escalation, this is not always the case. As with other process parameters, there is a threshold after which mechanisms of carbonation other than the CO₂ dissolution become the limiting ones. For instance, above the optimum pressure, pH conditions that are not favorable for further carbonation may be created. Also, by implementing higher CO₂ pressures, the precipitation of carbonates and silicates accelerates, up to a point, and the formation of the passivating layer around the particles accelerates, thus hindering further carbonation.

Liquid-to-solid ratio: Chang et al.⁴⁴, van Zomeren et al.⁴⁵ and Baciocchi et al.⁴⁷ investigated the influence of the L/S ratio on the carbonation extent. Chang et al.⁴⁴ tested the influence of L/S ratio on the slurry carbonation of BOF slag. The authors found the optimal L/S ratio at 20

L/kg. For both lower and higher values than the optimal, the conversion extent decreased. For ratios below the optimal, the slurry did not mix well in the reactor causing poor mass transfer, whereas for ratios above the optimal, the excess liquid in the slurry led to a lower ionic strength.

van Zomeren et al.⁴⁵ and Baciocchi et al.⁴⁷ used two different regimes regarding the L/S ratio: one with lower L/S ratio (0.1 L/kg and 0.3 L/kg, respectively) and another with higher L/S ratio (2 L/kg and 5 L/kg, respectively). In both cases, it was found that increasing the L/S ratio led to higher CO₂ uptakes. The combination of saturation conditions with mechanical mixing aids in mass transfer between phases, and additional liquid allows more CO₂ and Ca²⁺ to be in solution at a given time, accelerating the reaction.

CO₂ Concentration: Polettini et al.⁴⁶ and Baciocchi et al.⁴⁷ examined the effect of gaseous CO₂ concentration on the carbonation of BOF slag. Both groups used three different percentages of gaseous CO₂ (10%, 40% and 100%) for the carbonation of the slag. Polettini et al.⁴⁶ investigated the slurry carbonation of BOF slag. According to their findings, CO₂ concentration had a marginal effect on carbonation conversion compared to temperature and total pressure. That is, a diluted gas once pressurized (up to 10 bar tested) yielded results as good as pure CO₂. Only at low total pressures (1 bar), higher CO₂ concentrations resulted in higher CO₂ uptakes. Baciocchi et al.⁴⁷ examined both wet and slurry routes of BOF carbonation. It was found that, for both routes, higher CO₂ concentrations, at fixed total pressure, led to significantly greater CO₂ uptakes, especially when comparing 10% to higher concentrations. The authors did not address the particularly low conversions achieved at 10%, which are at odds with the results of Polettini et al.⁴⁶

CO₂ flow rate: Chang et al.^{42,43} investigated the effect of gas flow rate on the slurry carbonation of BOF slag in a bubbling column where the slag circulated in the fluidized regime. Excessive flow rate values were found to cause a channeling effect in the slurry

reactor, compromising proper gas-liquid mass transfer and leading to a moderate decrease of carbonation conversion. The channeling effect at high flow rates was observed in both studies, and a trend of conversion extent decrease with increasing flow rate was noted in both works. Therefore, it was concluded that in such a reactor, the flow rate of CO₂-containing gas should be limited to that which supports satisfactory fluidization, but no higher. In pressurized reactors, as used in other studies, flow rate is not an issue, as long as CO₂ is continually supplied to maintain the required partial pressure.

Slurry flow rate: Chang et al.⁴⁴ studied the influence of slurry flow rate on the carbonation conversion rate of BOF slag using a rotating packed bed reactor. According to the authors, an increase in the slurry flow rate improved the radial velocity of the slurry particles. Therefore, the mass transfer between the slurry and the gas phase, and the micro-mixing within the slurry, were significantly enhanced. As a result, the conversion rate was initially increased. However, further increase of the slurry flow rate above an optimal value (1.2 L/min in this case) caused a decrease of the carbonation rate, mainly due to the limited residence time of the slurry in the packed zone of the reactor.

Stirring/rotation speed: the speed of stirring and rotation of slurry reactors, and its influence on the conversion rate, were respectively tested by Huijgen et al.⁴¹ and Chang et al.⁴⁴ The enhancement of the mixing/rotation speed initially improved both the mass transfer between the CO₂ and the slurry, and the Ca²⁺ diffusion from the slag particles into the solution. In both studies there was an optimum speed (500 rpm for the reactor used by Huijgen et al.⁴¹ and 1000 rpm for the reactor used by Chang et al.⁴⁴) up to which, the conversion rate increased. A further increase of the speed over these optimal values caused a decrease in the conversion rate mainly due to the limited residence time of the slurry in the packing zone of the reactor,⁴⁴ or did not show any statistically appreciable improvement.⁴¹ Above a certain mixing rate, particle abrasion may aid in carbonation rate and conversion,⁴⁹ but the increased energy

expenditure and processing cost may not be worth the improvement from a CO₂ sequestration point of view.

Slurry volume and steam addition: in addition to the above parameters, slurry volume, in a bubbling fluidized column, was tested by Chang et al.⁴³ and steam addition during the direct dry carbonation of BOF slag was tested by Santos et al.⁴⁸ In the work of Chang et al.⁴³, the conversion increased with increasing slurry volume, at constant L/S ratio and gas flow rate, up to a certain value (350 mL). Due to the higher slurry volume the retention time of the CO₂ gas in the reactor (which was continuously supplied and removed) increased, and the conversion extent increased accordingly. For greater volumes the conversion decreased. This was hypothesized to be the result of poor mixing between the liquid and the solid phase of the greater volume of slurry, under constant gas flow rate (i.e., fluidization was less effective).

The addition of steam had a positive effect on the CO₂ uptake for all particle sizes tested by Santos et al.⁴⁸ However, its influence on the CO₂ uptake was reduced for larger sizes. The exact mechanism that leads to this positive influence is not fully understood, and could be related to a catalytic or mass transfer effect. The most convincing theory is that the addition of steam into the reactor improves the solid state diffusion of the CO₂ into the solid particles. However, further research is needed to confirm the exact mechanism that causes this improvement of the solid state diffusion.

2.3. Electric arc furnace (EAF) and stainless steel (SS) slags

Electric arc furnace slags are generated and extracted during the operation of electric arc furnaces as part of the steel-making process. On some occasions, stainless steel slag is denominated as a mixture of EAF slag and argon-oxygen decarburization (AOD) slag generated during the production of alloy steel. The wet carbonation of both the EAF and SS slags, as well as the slurry carbonation of the EAF slag have been studied by Baciocchi et

al.^{38,49} The effects of temperature, reaction time, CO₂ pressure, L/S ratio and particle size on the carbonation rate and conversion were tested, as discussed next.

Temperature: increased reaction temperature enhances dissolution of the silicates. Consequently, the wet carbonation of both EAF and SS slags improves with temperature enhancement. However, the extent of the tested temperature was limited up to 50 °C, and the carbonation behavior towards higher temperatures was not reported.

Particle size: milling of EAF and SS slag particles resulted in significant improvement of carbonation extent due to the increase of the specific surface area. These findings are consistent with those achieved in the previous studies related to the BF⁴⁰ and BOF slags.^{33,41-}

44,48

Reaction time: After an initial period during which the wet carbonation extent increased with decreasing rate, it leveled off. This finding agrees with those reported in previous studies related to BF and BOF slags. The main reason for this effect is the precipitation of the newly formed CaCO₃ that eventually blocks the pores of the slag particles and prevents the diffusion of the silicates from the solid slag particle to the solution.

Liquid-to-solid ratio: the optimal L/S ratio was found to be 0.4 L/kg. For both lower and higher ratios than the optimal, the conversion decreased. The authors commented on the rather high L/S ratio value for a wet carbonation process. They suggested that differences between this and other studies could be attributed to the slag's composition lacking hydrated lime, which would increase the water needed for hydration of the oxide and silicate phases, besides for dissolution of CO₂ and Ca²⁺ ions. The study with which Baciocchi et al.^{38,49} made the comparison was that of Johnson et al.,⁵⁰ who studied the influence of carbonation on the strength of EAF slag, and reported an optimal L/S ratio of 0.125 L/kg. It should be noted, however, that Johnson et al.⁵⁰ were optimizing the compressive strength of carbonated

compacts, so the L/S ratio was likely optimized not only in view of maximal carbonation conversion but also the physical characteristics of the post-carbonation compacts.

CO₂ pressure: the partial pressure of CO₂ had insignificant influence on the extent of the wet carbonation of EAF or SS slag, as reported by Baciocchi et al.^{38,49} for values between 1 and 10 bar CO₂. Only in the case of the EAF slag was it found that, for reaction times less than one hour, the increase of pressure from 1 to 3 bar produced a 43% enhancement of the CO₂ uptake.

2.4 Argon oxygen decarburization (AOD) and continuous casting (CC) slags

Argon-oxygen decarburization and continuous casting slags are generated in the refining step of the steel-making process. Carbonation of AOD and CC slags has been studied by Baciocchi et al.³⁸ using a pressurized stainless steel reactor, Vandeveld⁵¹ using a CO₂ incubator, Santos et al.^{39,52} using an ultrasound-assisted beaker, a CO₂ incubator and an autoclave reactor, and Van Bouwel⁵³ using an autoclave reactor. The effects of temperature, reaction time, CO₂ pressure, L/S ratio, particle size and sonication on carbonation conversion and rate of AOD and CC slags was investigated in these studies, and are discussed next.

Temperature: Vandeveld⁵¹ and Van Bouwel⁵³ studied the effect of temperature on the carbonation conversion of AOD and CC slags, following the wet and slurry routes, respectively. Vandeveld⁵¹ reported that for 30 °C and 50 °C, the lower temperature favored carbonation, achieving higher CO₂ uptakes after the first hour of reaction; after 6 hours of reaction time, however, both temperatures showed similar carbonation conversion. Vandeveld⁵¹ attributed this behavior to the increased solubility of CO₂ in the liquid film at lower temperatures (and while at low CO₂ partial pressures), which facilitated the transport of CO₂ to the reaction zone within the paste in the first stages of carbonation, before a passivating layer formed in the later stages, restricting access to the reaction front. Van

Bouwel⁵³ tested a wider range of temperatures, ranging between 30 °C and 180 °C, under pressurized conditions. The carbonation of AOD and CC slags behaved similarly to that observed during carbonation of the BF, BOF and EAF slags under raising temperatures, except for different optimal temperature. The optimum temperature for both AOD and CC slags was 60 °C. After this point, the reaction rate leveled off and the conversion extent remained constant at ~60%. The more amenable mineralogy of AOD and CC slags, consisting mainly of calcium silicates,³⁹ appears to make these slags more susceptible to carbonation at more moderate processing conditions.

Reaction Time: its impact on the carbonation extent of AOD and CC slags is reported by Santos et al.^{39,52}, Vandeveld⁵¹ and Van Bouwel.⁵³ In all the studies, the reaction time had similar impact on the conversion of AOD and CC slags. Regardless of the carbonation route that was used, carbonation extent increased with time, while carbonation rate decreased after an initial rapid period; carbonation extent eventually leveled off before reaction completion (based on chemical composition). This behavior is in agreement with that reported in studies related to BF, BOF and EAF slags, discussed earlier.

CO₂ Pressure: Baciocchi et al.,³⁸ Santos et al.,³⁹ and Van Bouwel⁵³ reported the effects of CO₂ partial pressure on the carbonation extent of AOD and CC slags. These studies pointed out a difference in behavior between AOD and CC slags towards increasing CO₂ partial pressure. Van Bouwel⁵³ showed CC slag starting with a high conversion extent at low partial pressure. With increasing partial pressure, the conversion extent dropped until 20 bar. After that point, further increase of the CO₂ pressure (up to 30 bar) led to a steep increase of the carbonation extent. AOD slag, on the other hand, showed a different behavior. Up to 12 bar, the pressure did not have any significant impact on the conversion extent of the slag, whereas after that point any further increase of the CO₂ pressure (up to 30 bar) led to a steep increase of the carbonation extent. Slightly different trends were reported by Santos et al.³⁹ In that

particular work, CC slag experienced an initial enhancement of conversion extent with increasing CO₂ pressure up to 9 bar. With further increase of the partial pressure, the conversion extent dropped until 13 bar. After that point, further increase of the CO₂ pressure (up to 30 bar) led to a steep increase of the conversion extent. The conversion extent of AOD slag appeared to be enhanced with increasing CO₂ pressure, and peaked at 20 bar. Any further increase of the partial pressure (up to 30 bar) did not seem to significantly affect the conversion extent.

Baciocchi et al.³⁸ studied the wet carbonation of AOD slag. In this study, the effect of CO₂ partial pressure on the carbonation conversion of AOD slag was examined as a function of reaction time. It was evident that the effect of the increasing partial pressure became more significant after the initial period (2 h) of carbonation. This agrees with the findings for the other slags discussed earlier. The CO₂ pressure increase facilitates the diffusion of ions through the passivating layers (precipitated carbonate and residual silica) that are formed and thicken during carbonation.⁵²

L/S ratio: in the case of AOD⁵³ and CC^{39,51,53} slags, there was an optimal value for the L/S ratio. For both lower and higher values than the optimal, the carbonation conversion decreased. For solids loading values below the optimal (i.e., high L/S ratio), particle attrition is reduced in agitated slurry systems, while a mass transfer barrier (thick diffusion boundary layer) is created due to the excessive water in wet (thin-film) systems. For solid loading values above the optimal (i.e., low L/S ratio), the slurry did not mix well within the reactor, causing poor contact between the reacting particles and the carbonic acid solution, leading to slow carbonation rates and low carbonation conversions. This is consistent with the findings of the previously discussed studies related to the L/S ratios of the wet and slurry carbonation of BF, BOF and EAF slags.

Sonication: Santos et al.⁵² conducted carbonation experiments with sonication in order to intensify the carbonation extent of AOD and CC slags. The results of this study indicated that ultrasound usage significantly enhanced the carbonation conversion of both slags. The implementation of sonication in the carbonation experiments resulted in enhanced solid-liquid-gas mixing, and consequently better mass transfer as well as enhanced CO₂ dissolution, which are significant parameters for the carbonation process. Removal of the passivating layers that surrounds the unreacted inner part of the particle via sonication intensified the reaction rate and sustained the reaction until higher conversion levels were reached. Sonication also resulted in the breakage of slag particles themselves, leading to higher specific surface area of the particles, and thus improved reactivity.

Mineralogy: for all reported studies, the conversions achieved by CC slag are notably higher than those of AOD slag, under similar conditions. This has been identified as being due to the more favorable mineralogy of CC slags,³⁹ which contain considerably higher amounts of gamma-dicalcium-silicate (γ -C₂S) than AOD slags, which in turn are richer in β -C₂S. Chang et al.⁵⁴ recently proposed, based on nuclear magnetic resonance studies, that the structural environment of silicon in γ -C₂S leads to easier protonation of SiO₄⁴⁻ groups (and thus easier decalcification), based on the predominant monomeric structure (Q⁰) of silica in the carbonated mineral.

2.5 Waelz slag

Waelz slag is a by-product of the Waelz process which recovers zinc, mainly from EAF slag, by using a rotary kiln. The material that is left after zinc recovery is called Waelz slag. Cappai et al.⁵⁵ studied the influence of three parameters on the carbonation extent and rate of Waelz slags, under constant temperature (25 °C): reaction time, CO₂ partial pressure, and L/S ratio.

Reaction time: similar to the other types of slags, the conversion extent increased with decreasing rate as the reaction duration increased. The maximum carbonation extent was achieved after 240 hours of reaction.⁵⁵

CO₂ pressure: generally, conversion extent was enhanced with increasing CO₂ pressure.⁵⁵ The conversion extent enhancement was more evident after the first 24 hours of reaction. For shorter reaction times, CO₂ pressure did not appreciably affect the conversion extent. This is because the impact of pressure on carbonation extent becomes more pronounced after the formation of the initial passivating layers around the reacting particles. Higher CO₂ pressure facilitates the diffusion of ions through these layers.

L/S ratio: the carbonation kinetics appeared to be strongly influenced by the L/S ratio.⁵⁵ As expected, at L/S = 0, the kinetics were very slow, since hydration aids in the mobility, and thus reactivity, of ions within the solid minerals. By gradually increasing the L/S ratio up to 1 L/kg, the reaction rate became significantly faster. Accordingly, the carbonation extent at lower L/S ratios was notably less than that at higher ratios.

3. CARBONATION WEATHERING RATE (CWR): CONCEPTUALIZATION AND APPLICATION

Although several studies on steel-making slag carbonation have been conducted, comparison of their reported reaction rate and conversion extent results has proven challenging. The main reason for this is that the slags used by the researchers have different particles sizes, and thus different specific surface areas. Mineral carbonation is a solid-state-diffusion-limited process under most conditions, so the different particle sizes affect the carbonation rate and maximal achievable conversion. In order to make direct comparisons among the results obtained from different studies, the CWR is conceptualized. The rate is expressed in units of $\mu\text{m}\cdot\text{min}^{-1}$, and

represents the weathering rate of the particle radius from the original outer radius to the final radius of the unreacted core of the carbonated particle.

The CWR assumes that all reactive minerals carbonate at similar rates, that all particles are spherical, and does not account for the changing size of particles due to the accumulation of precipitated carbonates on the particle;⁵² that is, it only tracks the location of the reacted | unreacted interface. The first assumption is supported by research: the study of Bodor et al.⁵⁶, who synthesized different alkaline minerals and carbonated them, showed that carbonation kinetics and extent differ but not substantially for the most abundant minerals found in iron- and steel-making slag. The second assumption is in principle not as accurate, since the aspect ratio of iron- and steel-making slag particles is sometimes relatively high.⁵² However, laser diffraction is the typical technique used for determining average particle size, and this method does not distinguish particle shapes;⁵⁷ therefore the values used in the calculation of the CWR are already assumed to represent spherical particles. The third assumption, not tracking the outer edge of the particle, simply implies that the length unit of the CWR relates to the radius of the original average particle.

One limitation of the CWR is that it does not differentiate between weathering rate improvement due to particle size reduction and particle porosity enhancement. Thus, if a material is mechanically activated to improve carbonation, it will not be possible to distinguish between the two effects based on how the CWR responds. Another aspect to bear in mind is that the CWR can either represent the average weathering rate over the duration of a carbonation process, or it can be taken as an instantaneous snapshot at any point in time during carbonation. It would be expected that the CWR would be greater initially, and reduce as time passes, due to the nature of the shrinking core model. A carbonation process can, in principle, operate near peak-CWR if CO₂ sequestration is the main goal, and mineral acquisition and handling costs are rather low. However, if mineral valorization or treatment is

also a goal, the carbonation process would be designed to operate at lower overall CWR by increasing processing duration, to achieve required final material properties for commercialization or safe disposal.

The first step in calculating the CWR is to obtain the average radius of the unreacted core of mineral particles (R), using Eqn (4) for the average particle conversion degree ($C\%$), where $C\% \leq 100\%$. The value of $C\%$ is typically experimentally obtained by researchers via thermogravimetric analysis or quantitative X-ray crystallography.

$$C\% = \frac{\frac{4}{3}\pi r_x^3 - \frac{4}{3}\pi R^3}{\frac{4}{3}\pi r_x^3} \cdot 100\% = \frac{r_x^3 - R^3}{r_x^3} \cdot 100\% \quad (4)$$

As illustrated in Figure 1, based on the aforementioned assumptions, r_x is the original average particle radius, and R is the average radius of the unreacted core of the particle. It should be noted if the particle size distribution is known, it is possible to apply this equation to each particle size fraction and solve for a single value of R ; the particle with $r_x = R$ would be the largest particle that carbonates fully (within the bounds of the assumptions made).⁵⁸

Based on Eqn (4) and knowing that $R = (r_x - t_{carb})$, where t_{carb} is the thickness of the carbonated shell of the particle (Fig. 1), it is possible to calculate the value of t_{carb} by using the following solution (Eqn (5)):

$$t_{carb} = r_x \cdot \left(1 - \sqrt[3]{1 - C\%/100\%}\right) \quad (5)$$

For example, if the conversion is complete ($C\% = 100\%$), then t_{carb} will be equal to r_x , meaning the whole particle becomes a carbonate sphere. If the conversion is half ($C\% = 50\%$), the thickness of the carbonated shell will be 20.6% of the original particle radius, since the radius of a sphere half the volume of a larger sphere is 79.4% of the larger sphere's radius. By knowing both t_{carb} , for a given $C\%$, and the reaction time (τ_{react}) that is required to

reach the $C\%$, it is possible to calculate the CWR (Eqn (6)), which is essentially the t_{carb} normalized per unit time:

$$CWR = \frac{t_{carb}}{\tau_{react}} = \frac{r_x \cdot \left(1 - \sqrt[3]{1 - C\%/100\%}\right)}{\tau_{react}} \quad (6)$$

By applying Eqn (6) to the conversions achieved by the studies that have been reviewed in this paper, Table 3 is created. Some studies refer to the size of the slag particles as a range instead of a specific average mean diameter. In those cases, an arithmetic average of the range was taken as the mean diameter. Figures 2, 3, and 4 indicate the CWR s of the reported studies on BOF, AOD, and CC slags, respectively, in chronological order. Figure 5 indicates the CWR s of studies on SS, EAF, BF, and Waelz slags.

As an overall observation, it is clearly shown that the highest carbonation conversions do not necessarily correspond to the highest CWR s. In fact, the CWR values present a totally different distribution among the different studies than in the case of conversions. The highest CWR ($0.618 \mu\text{m}/\text{min}$) originates from the carbonation of the BOF slag under mild conditions ($T = 65 \text{ }^\circ\text{C}$, $P_{\text{CO}_2} = 1 \text{ bar}$, L/S ratio of 20 L/kg , CO_2 flow rate equal to 1.2 L/min , and an average particle diameter of $62 \mu\text{m}$), as studied by Chang et al.⁴⁴ The same study also presents the highest carbonation conversion (93.5%). However, this is not the case for the rest of the studies. The next most effective experimental studies are those of Huijgen et al.⁴¹, followed by Tai et al.³³, who carbonated BOF and BF steelmaking slag, respectively. By using the CWR value, it is shown that the setups used resulted in CWR values equal to $0.229 \mu\text{m}/\text{min}$ and $0.188 \mu\text{m}/\text{min}$, respectively. However, in terms of conversion extents achieved, these studies present remarkably lower values in comparison with others. This is either because the particles used were too large to enable high levels of conversion, or because the reactions were not run for sufficient time to allow high conversions to be reached, or because different slags have different carbonation kinetics, due to differences in mineralogy (some

minerals are more reactive than others) or morphology (some slags are more or less porous, or become more or less porous during reaction) differences.

CWR values are most applicable for comparing results obtained for the same type of iron- or steel-making slag, as then the only barrier to the effective comparison among conversions resulting from different studies is the particles size. In the case of BOF slags, it is shown that the rate of carbonation weathering achieved by Chang et al.⁴⁴ is clearly the highest, followed by Huijgen et al.⁴¹ (0.229 $\mu\text{m}/\text{min}$) and Santos et al.⁵² (0.184 $\mu\text{m}/\text{min}$). As far as the AOD and CC slags are concerned, Van Bouwel⁵³ has the higher CWRs for both of these types of slag, with 0.108 and 0.124 $\mu\text{m}/\text{min}$, respectively. Furthermore, similar to the carbonation conversions, the CWR value is higher for CC slag than AOD slag. Santos⁵⁸ points out that in addition to mineralogy, the particle size difference between the two slags, which are naturally comminuted, can explain the differences in carbonation rate and conversion. With the CWR value, these differences are innately considered.

It is worthwhile to point out the EAF slag study conducted by Baciocchi et al.³⁶ It is one of the few cases in the literature where wet (thin-film) carbonation of a particular slag results in higher conversion extent than when using the slurry route. However, the CWR that results from the wet route is remarkably lower than that from the slurry route (0.010 $\mu\text{m}/\text{min}$ for wet carbonation, versus 0.046 $\mu\text{m}/\text{min}$ for slurry carbonation), indicating that the slurry route is the more time-efficient way for carbonation. In fact, the higher conversion that was achieved by the wet route could be attributed to the longer period of carbonation (6 days vs. 6 hours). This comparison confirms the usefulness of the CWR measure in delivering more accurate and insightful results as opposed to simple CO_2 uptake or conversion extent, since the CWR takes the reaction period into consideration, in addition to the particle size.

4. CONCLUSIONS

Slags from the steel-making process are characterized by a remarkable ability for CO₂ fixation in a permanent manner by forming carbonate minerals that can permanently remain stable, from a thermodynamic aspect. Although their ability to store a significant fraction of anthropogenic CO₂ emissions is limited (due to relatively limited availability of the material), steel-making slags are capable of storing meaningful quantities of CO₂ emitted by the iron- and steel-making industries. The influence of several operational parameters on the carbonation rate and conversion extent of iron- and steel-making slags has been thoroughly examined in this review. General trends for the influence of each operational parameter were obtained, and seen to be largely in agreement among the various studies, despite the variations in the slag types, and consequently composition and morphology, and carbonation process used in the different studies.

The influence of the four main experimental parameters on iron- and steel-making slag carbonation can be outlined as follows:

Temperature: the carbonation process consists of three different mechanisms: Ca²⁺ diffusion from the solid particle, CO₂ dissolution into the aqueous solution, and carbonate nucleation. Each mechanism has a different response to temperature alterations. Temperature increase enhances Ca²⁺ leaching from the solid matrix, but attenuates CO₂ dissolution. Consequently, two main regimes are observed regarding the influence of temperature on carbonation conversion of iron- and steel-making slags. Increasing temperature up to an optimal value enhances the reaction rate and conversion extent, whereas further increase of the reaction temperature ultimately hinders the conversion.

Particle size: decreasing the slag's particle size enhances carbonation conversion as direct mineral carbonation is a surface-based reaction. The conceptualized CWR removes the effect of particle size from conversion data, allowing better comparison of different works based on the carbonation processes used.

Reaction time: the increase of the reaction time improves the carbonation extent, but carbonation rate is attenuated as time passes, due to particle passivation. However, after a certain period, the carbonation conversion levels off as the passivation layer becomes impenetrable, or poorly reactive alkaline minerals do not respond to carbonation at the utilized process conditions. The conceptualized CWR normalizes carbonation conversion data based on time, thus allowing better comparison between the effectiveness of different carbonation processes on the rate of CO₂ uptake.

Liquid-to-solid ratio: too high or too low values of L/S ratio are detrimental to mineral carbonation; dry-out conditions hinder reactivity, while dilute conditions diminish particle-particle abrasion in mixed systems, and enlarge diffusion boundary layers in stationary systems. L/S ratio must be optimized for each case, based on the type of the material that is used and the type of carbonation process that is implemented.

Out of the 19 studies covered in this review, the average CWR was 0.08 µm/min. This means that a slag particle 10 µm in diameter fully carbonates, on average, in roughly one hour, whereas a slag particle 100 µm in diameter typically takes in the order of 10 hours to achieve full carbonation, disregarding mineralogical or morphological impediments and any intensification technique used (e.g., sonication⁵² or mechanical attrition⁴⁴). This type of estimate is useful when considering industrialization of mineral carbonation as a means of CO₂ sequestration. It provides process designers a reasonable idea of the sort of reactor scale needed and logistics involved in sequestering CO₂ from flue gas emissions, depending on the rate of emissions and sequestration target, and the level of comminution needed to turn iron- or steel-making slag into a suitable carbon sink. Process intensification techniques are an option to accelerate mineral carbonation,³⁷ but the extra processing costs and energy demand introduced may not justify their application when the sole purpose of carbonation is CO₂ sequestration,⁵⁸ which requires a low-carbon-intensity process. Process intensification

strategies become useful if the CWR is augmented by one or more orders of magnitude. Chang et al.⁴⁴ managed to nearly achieve this, in comparison with the aforementioned average, with a CWR of 0.62 $\mu\text{m}/\text{min}$ for BOF slag carbonation in a high-gravity rotating packed bed.

5. REFERENCES

1. Tans P, Keeling R, Trends in Atmospheric Carbon Dioxide, NOAA/ESRL, <http://www.esrl.noaa.gov/gmd/ccgg/trends> (Accessed January 17, 2016).
2. Climate at a Glance, NOAA, <http://www.ncdc.noaa.gov/cag/time-series/global> (Accessed January 23, 2016).
3. Sherwood SC, Bony S and Dufresne JL. Spread in model climate sensitivity traced to atmospheric convective mixing. *Nature* **505**: 37–42 (2013).
4. European Commission, Climate Action, Paris Agreement, http://ec.europa.eu/clima/policies/international/negotiations/future/index_en.htm (Accessed January 17, 2016).
5. Taylor M. The current and future state of CCS and its deployment around the world. *Greenhouse Gases: Science & Technology* **2**: 399–401 (2012).
6. Johnsson F. Perspectives on CO₂ capture and storage. *Greenhouse Gases: Science & Technology* **1**: 119–133 (2011).
7. Petroleum Technology Research Centre, *What Happens When CO₂ is Stored Underground? Q&A from the IEAGHG Weyburn-Midale CO₂ Monitoring and Storage*

Project. Global Carbon Capture and Storage Institute Limited, Melbourne, Australia (2014).

8. Lackner K. A guide to CO₂ sequestration. *Science* **300(5626)**: 1677–1678 (2003).
9. Archer D. Fate of fossil fuel CO₂ in geologic time. *Journal of Geophysical Research* **110**: C09S05 (2005).
10. Prigiobbe V, Polettini A and Baciocchi R. Gas-solid carbonation kinetics of air pollution control residues for CO₂ storage. *Chemical Engineering Journal* **148(2-3)**: 270-278 (2009).
11. Winkler EM. Important agents of weathering for building and monumental stone. *Engineering Geology* **1(5)**: 381–400 (1966).
12. Seifritz W. CO₂ disposal by means of silicates. *Nature* **345(6275)**: 486 (1990).
13. Santos RM, Verbeeck W, Knops P, Rijnsburger K, Pontikes Y, Van Gerven T. Integrated mineral carbonation reactor technology for sustainable carbon dioxide sequestration: ‘CO₂ Energy Reactor’. *Energy Procedia* **37**: 5884–5891 (2013).
14. Moazzem S, Rasul MG, Khan MMK. Energy recovery opportunities from mineral carbonation process in coal fired power plant. *Applied Thermal Engineering* **51**: 281–291 (2013).
15. Teir S. *Fixation of carbon dioxide by producing carbonates from minerals and steelmaking slags, Ph.D. Thesis*. Helsinki University of Technology, Espoo, Finland (2008).
16. Lackner KS, Wendt CH, Butt DP, Joyce EL and Sharp DH. Carbon dioxide disposal in carbonate minerals. *Energy* **20(11)**: 1153-1170 (1995).

17. Goff F, Lackner KS. Carbon dioxide sequestering using ultramafic rocks. *Environmental Geoscience* **5(3)**: 89-101 (1998).
18. Bodor M, Santos RM, Van Gerven T, Vlad M. Recent developments and perspectives on the treatment of industrial wastes by mineral carbonation - a review. *Central European Journal of Engineering* **3(4)**: 566–584 (2013).
19. Allen DJ, Brent GF. Sequestering CO₂ by mineral carbonation: stability against acid rain exposure. *Environmental Science and Technology* **44(7)**: 2735–2739 (2010).
20. Bodor M, Santos RM, Cristea G, Salman M, Cizer Ö, Iacobescu RI, et al.. Laboratory investigation of carbonated BOF slag used as partial replacement of natural aggregate in cement mortars. *Cement and Concrete Composites* **65(1)**: 55–65 (2016).
21. Kirchofer A, Becker A, Brandt A, Wilcox J. CO₂ mitigation potential of mineral carbonation with industrial alkalinity sources in the United States. *Environmental Science and Technology* **47**: 7548–7554 (2013).
22. *The World Factbook 2013-14*. Central Intelligence Agency, Washington, United States (2013).
23. International Energy Agency (IEA). *Technology roadmap: Carbon capture and storage, 2013 Edition*. IEA, Paris, France (2013).
24. Santos, RM, Mertens G, Salman M, Cizer Ö, Van Gerven T. Comparative study of ageing, heat treatment and accelerated carbonation for stabilization of municipal solid waste incineration bottom ash in view of reducing regulated heavy metal/metalloid leaching. *Journal of Environmental Management* **128**: 807–821 (2013).

25. Costa G, Baciocchi R, Polettini A, Pomi R, Hills CD and Carey PJ. Current status and perspectives of accelerated carbonation processes on municipal waste combustion residues. *Environmental Monitoring and Assessment* **135(1-3)**: 55–75 (2007).
26. Proctor DM, Fehling KA, Shay EC, Wittenborn JL, Green JJ, Avent C, et al.. Physical and Chemical Characteristics of Blast Furnace, Basic Oxygen Furnace, and Electric Arc Furnace Steel Industry Slags. *Environmental Science and Technology* **34(8)**: 1576-1582 (2000).
27. Motz H, Geiseler J. Products of steel slags an opportunity to save natural resources. *Waste Management* **21(3)**: 285-293 (2001).
28. Shen H, Forsberg E. An overview of recovery of metals from slags. *Waste Management* **23(10)**: 933-949 (2003).
29. Van Oss, H. *Iron and Steel Slag*, U.S. Geological Survey, Mineral Commodities Summaries, USA (2016).
30. Eloneva S, Teir S, Salminen J, Fogelholm CJ and Zerenhoven R. Fixation of CO₂ by carbonating calcium derived from blast furnace slag. *Energy* **33(9)**: 1461-1467 (2008).
31. Stollarof JK, Lowry GV and Keith DW. Using CaO- and MgO-rich industrial waste streams for carbon sequestration. *Energy Conversion and Management* **46(5)**: 687-699 (2005).
32. Johnson DC. Accelerated carbonation of waste calcium silicate materials. *SCI Lecture Papers Series* **108**: 1-10 (2000).

33. Tai CI, Su CY, Chen YT, Shih SM, and Chien WC. Carbonation of natural rock and steel slag using supercritical carbon dioxide. *11th European meeting on supercritical fluids*. International Society for Advancement of Supercritical Fluids (ISASF), Barcelona (2008).
34. Huijgen WJJ, Comans RNJ, Carbon dioxide sequestration by mineral carbonation, Literature review update 2003-2004. ECN-C-05-022 (2005). Available online: <http://www.ecn.nl/docs/library/report/2005/c05022.pdf> (accessed 2016-05-11).
35. Monkman S, Shao Y. Assessing the carbonation behavior of cementitious materials. *Journal of Materials in Civil Engineering* **18(6)**: 768-777 (2006).
36. Baciocchi R, Costa G, Di Bartolomeo E, Polettini A and Pomi R. Wet versus slurry carbonation of EAF steel slag. *Greenhouse Gases: science and technology* **1(4)**: 312-319 (2011).
37. Santos RM, Francois D, Vandeveld E, Mertens G, Elsen J and Van Gerven T (2011), Process intensification routes for mineral carbonation. *Greenhouse Gas: Science and Technology* **1(4)**: 287-293 (2011).
38. Baciocchi R, Costa G, Di Bartolomeo E, Polettini A and Pomi R. Carbonation of Stainless Steel Slag as a Process for CO₂ Storage and Slag Valorization. *Waste and Biomass Valorization* **1(4)**: 467-477 (2010).
39. Santos RM, Van Bouwel J, Vandeveld E, Mertens G, Elsen J and Van Gerven T. Accelerated mineral carbonation of stainless steel slags for CO₂ storage and waste valorization: Effect of process parameters on geochemical properties. *International Journal of Greenhouse Gas Control* **17**: 32-45 (2013).

40. Chang EE, Pan SY, Chen YH, Chu HW, Wang CF and Chiang PC. CO₂ sequestration by carbonation of steelmaking slags in an autoclave reactor. *Journal of Hazardous materials* **195**:107-114 (2011b).
41. Huijgen WJJ, Comans RNJ and Witkamp GJ. Mineral CO₂ sequestration by steel slag carbonation. *Environmental Science and Technology* **39(24)**: 9676-9682 (2005).
42. Chang EE, Chen CH, Chen YH, Pan SY and Chiang PC. Performance evaluation for carbonation of steel-making slags in a slurry reactor. *Journal of Hazardous Materials* **186(1)**: 558-564 (2011a).
43. Chang EE, Chiu AC, Pan SY, Chen YH, Tand CS and Chiang PC. Carbonation of basic oxygen furnace slag with metalworking wastewater in a slurry reactor. *International Journal of Greenhouse Gas Control* **12**: 382-389 (2013).
44. Chang EE, Pan SY, Chen YH, Tan CS and Chiang PC. Accelerated carbonation of steelmaking slags in a high-gravity rotating packed bed. *Journal of Hazardous Materials* **227-228**: 97-106 (2012).
45. van Zomeren A, van der Laan SR, Kobesen HBA, Huijgen WJJ et al. Changes in mineralogical and leaching properties of converter steel slag resulting from accelerated carbonation at low CO₂ pressure, *Waste Management* **31**: 2236-2244 (2011).
46. Polettini A, Pomi R, and Stramazzo A. Carbon sequestration via steel slag accelerated carbonation: the influence of operating conditions on process evolution and yield, *Proceedings of the 5th International Conference on Accelerated Carbonation for Environmental and Material Engineering (ACEME)*, New York, USA, 2015

47. Baciocchi R, Costa G, Polettini A, Pomi R, Stramazzo A and Zingaretti D.
Accelerated carbonation of steel slags using CO₂ diluted sources: CO₂ uptakes and energy requirements, *Proceedings of the 5th International Conference on Accelerated Carbonation for Environmental and Material Engineering (ACEME)*, New York, USA, 2015
48. Santos RM, Ling D, Sarvaramini A, Guo M, Elsen J, Larachi F, Beaudoin G, Blanpain B, Van Gerven T (2012), Stabilization of basic oxygen furnace slag by hot-stage carbonation treatment. *Chemical Engineering Journal* **203**: 239-250 (2012).
49. Baciocchi R, Costa G, Polettini A and Pomi R. Influence of particle size on the carbonation of stainless steel slag for CO₂ storage. *Energy Procedia* **1(1)**: 4859-4866 (2009).
50. Johnson DC, McLeod CL, Carey PJ and Hills CD. Solidification of stainless steel slag by accelerated carbonation. *Environmental Technology* **24(6)**: 671-678 (2003).
51. Vandeveld E. *Mineral carbonation of stainless steel slag, Master's Thesis*, KU Leuven, Leuven, Belgium, 2010.
52. Santos RM, François D, Mertens G, Elsen J, Van Gerven T. Ultrasound-intensified mineral carbonation. *Applied Thermal Engineering* **57(1-2)**: 154-163 (2012).
53. Van Bouwel J. *Intensified aqueous mineral carbonation of alkaline industrial residues for CO₂ storage and waste remediation: effect of process parameters on carbonation conversion, leaching behavior and mineralogy, Master's Thesis*, KU Leuven, Leuven, Belgium, 2012.

54. Chang J, Fang Y, Shang X. The role of β -C₂S and γ -C₂S in carbon capture and strength development. *Materials and Structures* (in press) doi:10.1617/s11527-016-0797-5.
55. Cappai G, De Giudici G, Medas D, Muntoni A, Nieddu A, Orrù G, Piredda M. Carbon dioxide sequestration by accelerated carbonation of Waelz slag, *Proceedings of the 5th International Conference on Accelerated Carbonation for Environmental and Material Engineering (ACEME)*, New York, USA, 2015.
56. Bodor M, Santos RM, Kriskova L, Elsen J, Vlad M, Van Gerven T. Susceptibility of mineral phases of steel slags towards carbonation: Mineralogical, morphological and chemical assessment. *European Journal of Mineralogy* **25**(4): 533-549 (2013).
57. Tinke AP, Carnicer A, Govoreanu R, Scheltjens G, Lauwerysen L, Mertens N, Vanhoutte K, Brewster ME. Particle shape and orientation in laser diffraction and static image analysis size distribution analysis of micrometer sized rectangular particles. *Powder Technology* **186**: 154-167 (2008).
58. Santos RM. *Sustainable materialization of residues from thermal processes into carbon sinks, PhD Thesis*, KU Leuven, Leuven, Belgium, 2012.

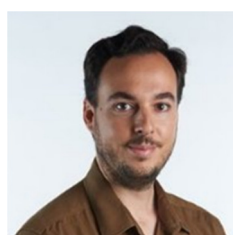
Biographies:

Evangelos Georgakopoulos



Evangelos Georgakopoulos is a doctoral researcher at the Cranfield University, School of Engineering. He is working on mineral carbonation and industrial waste (steel slag) valorization. He holds a BSc degree (Geology and Geoenvironment) from the National and Kapodistrian University of Athens and an MSc degree (Renewable Energy Enterprise & Management) from Newcastle University.

Rafael Mattos dos Santos



Rafael Mattos dos Santos is Professor of Applied Chemical and Environmental Sciences at the Sheridan Institute of Technology. He is co-founder of the Sheridan Chemical and Environmental Laboratories (CEL). His expertise portfolio includes mineral carbonation and process intensification. He holds BSc and MSc (Chemical Engineering) degrees from the University of Toronto, a PhD degree (Chemical Engineering) from the KU Leuven, and is a registered Professional Engineer of Ontario.

Yi Wai Chiang



Yi Wai Chiang is Assistant Professor in the School of Engineering at the University of Guelph. She is co-founder of the Advanced Materials Characterization Consortium. Her expertise portfolio includes waste valorization and bioengineering. He holds BSc and MSc

(Chemical Engineering) degrees from the University of Toronto, a PhD degree (Bioscience Engineering) from the KU Leuven, and is a registered Professional Engineer of Ontario.

Vasilije Manovic



Vasilije Manovic is Professor of Carbon Systems Engineering at the Centre for Combustion, Carbon Capture & Storage at Cranfield University. He is an internationally recognized authority in several CO₂ capture technologies, including calcium looping, chemical looping combustion, and oxy-fuel combustion, and on CO₂ capture from low-CO₂-concentration sources. He holds a PhD degree (Chemistry) from the University of Belgrade.

List of Figures:

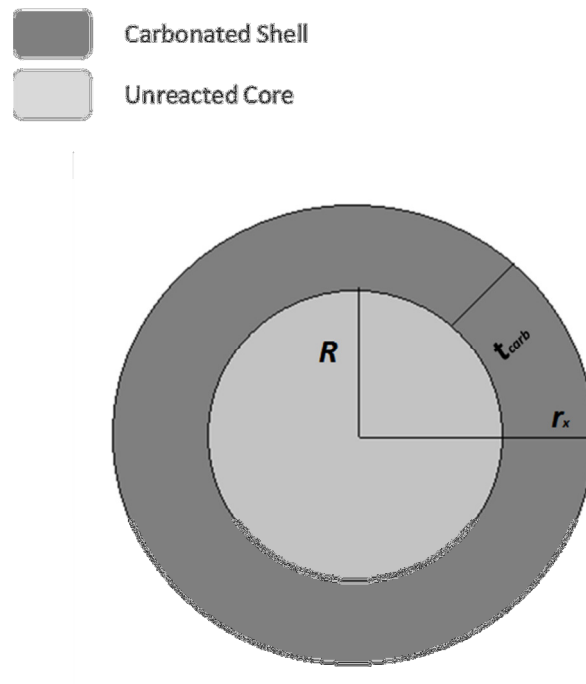


Figure 1. Theoretical illustration of a partially carbonated mineral particle.

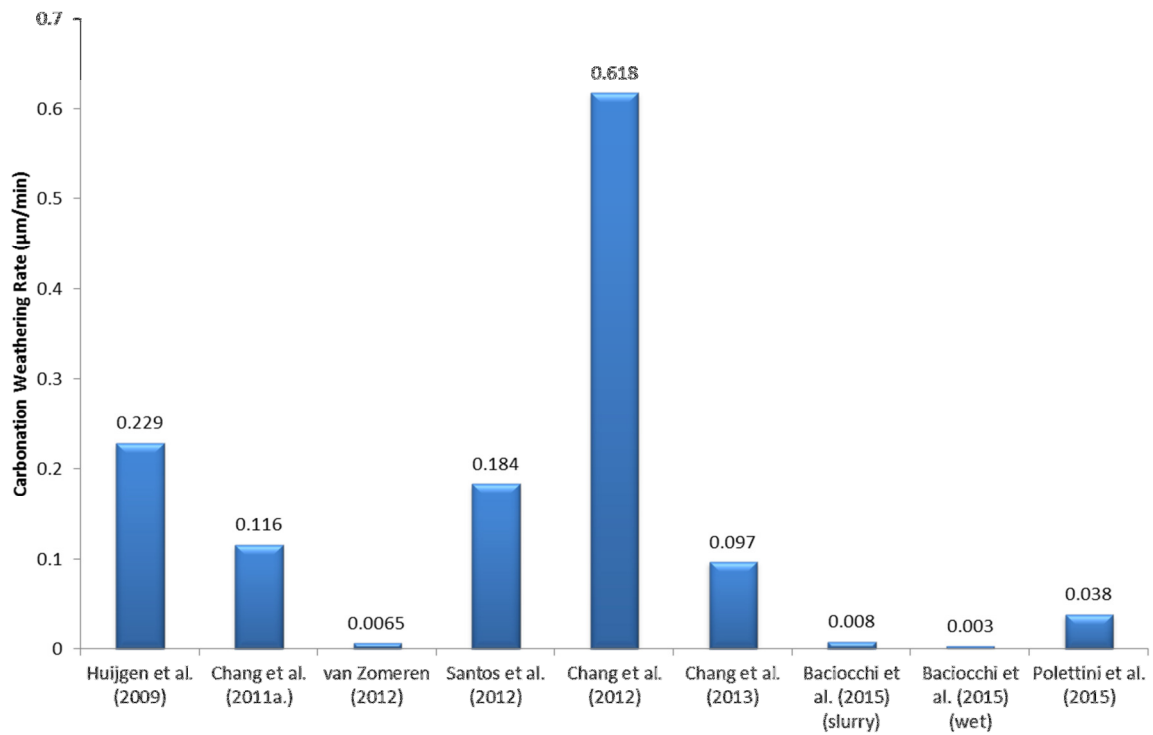


Figure 2. Carbonation Weathering Rates as calculated for studies on BOF slag.

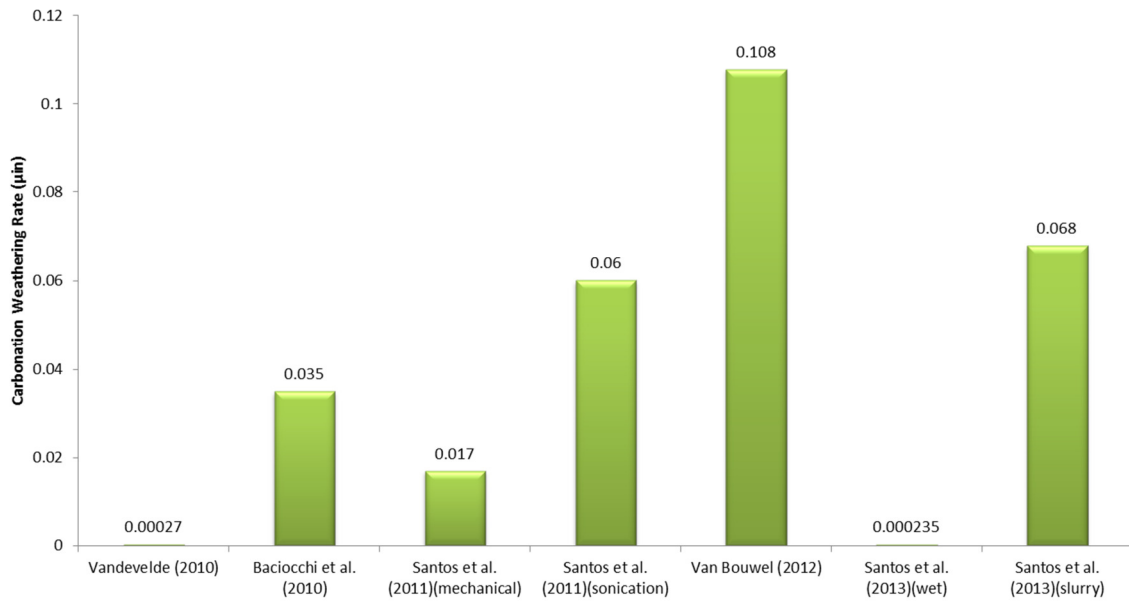


Figure 3. Carbonation Weathering Rates as calculated for studies on AOD slag.

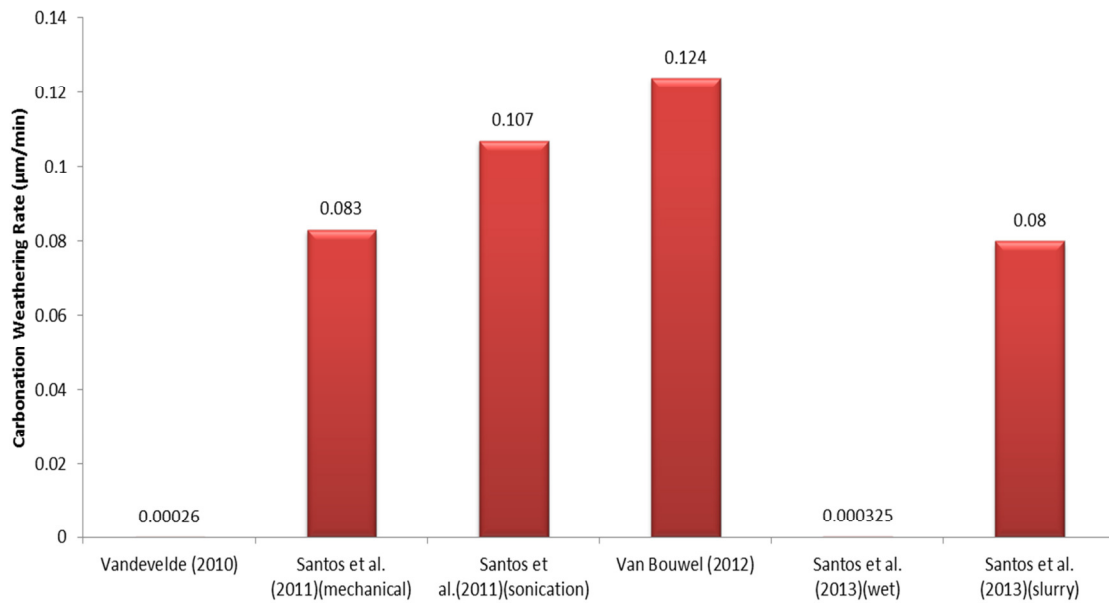


Figure 4. Carbonation Weathering Rates as calculated for studies on CC slag.

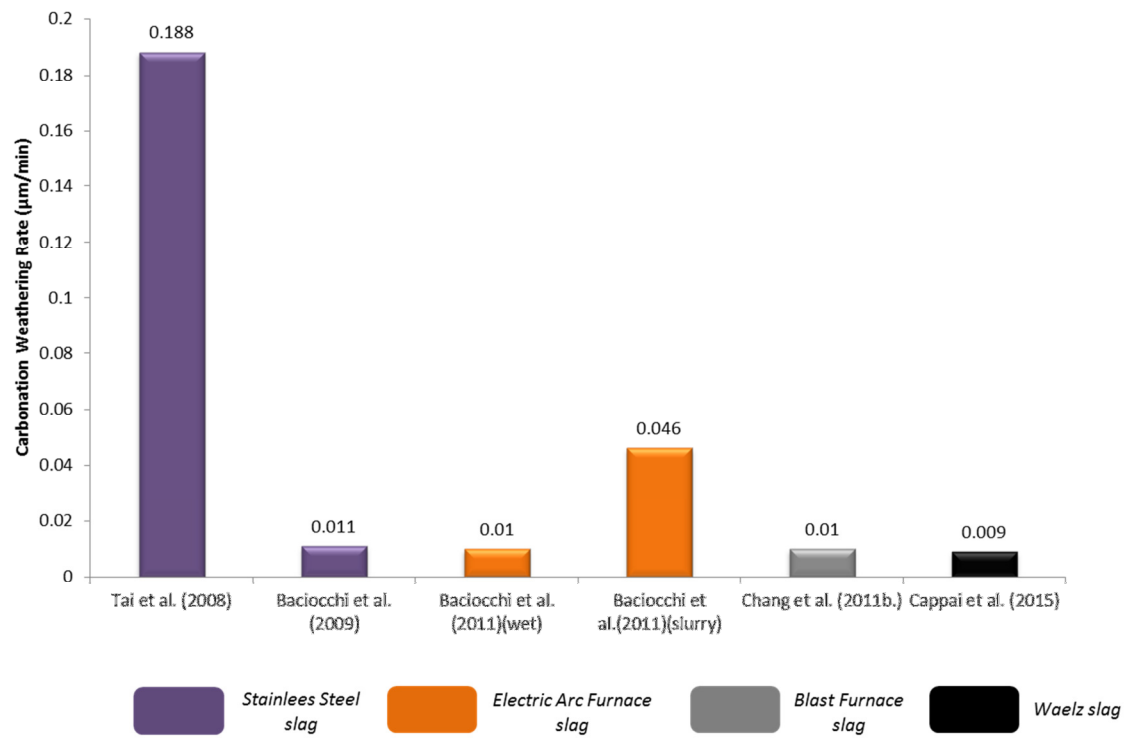


Figure 5. Carbonation Weathering Rates as calculated for studies on SS, EAF, BF, and Waelz slags.

List of Tables:

Table 1: Types of slags and reactors, and carbonation routes used in various carbonation studies.

Reference	Slag Type	Reactor Type	Carbonation Route
Huijgen et al. (2009) ⁴¹	BOF	Autoclave Reactor	Slurry Carbonation
Chang et al. (2011a) ⁴²	BOF	Column Slurry Reactor	Slurry Carbonation
Van Zomeren (2011) ⁴⁵	BOF	Column Reactor	Wet/Slurry Carbonation
Santos et al. (2012) ⁴⁸	BOF	TGA Reaction: crucible Pressurized Basket Reactor Atmospheric Furnace	Dry Carbonation
Chang et al. (2012) ⁴⁴	BOF	High-Gravity Rotating Packed Bed (RPB)	Slurry Carbonation
Chang et al. (2013) ⁴³	BOF	Column Slurry Reactor	Slurry Carbonation
Polettini et al. (2015) ⁴⁶	BOF	Pressurized Stainless Steel Reactor	Slurry Carbonation
Baclocchi et al. (2015) ⁴⁷	BOF	Pressurized Stainless Steel Reactor	Wet/Slurry Carbonation
Johnson et al. (2003) ⁵⁰	SS	Pressurized Sealed Chamber	Mold Carbonation
Tai et al. (2008) ³³	SS	Stirred High-Pressure Batch Reactor	Slurry Carbonation
Baclocchi et al. (2009) ⁴⁹	SS	Pressurized Stainless Steel Reactor	Wet Carbonation
Baclocchi et al. (2010) ³⁸	EAF, AOD	Pressurized Stainless Steel Reactor	Wet Carbonation
Baclocchi et al. (2011) ³⁶	EAF	Pressurized Stainless Steel Reactor	Slurry Carbonation
Vandeveld (2010) ⁵¹	AOD,CC	Pressurized Incubator Chamber	Wet Carbonation
Santos et al. (2011) ³⁷	AOD,CC	Common Glass Beaker	Slurry Carbonation
Van Bouwel (2012) ⁵³	AOD,CC	Autoclave Reactor	Slurry Carbonation
Santos et al. (2013) ³⁹	AOD, CC	Thin Film Reaction: Incubator Slurry Reaction: Autoclave Reactor	Thin Film Reaction: Wet Carbonation Slurry Reaction: Slurry Carbonation
Chang et al. (2011b) ⁴⁰	BF	Autoclave Reactor	Slurry Carbonation
Cappai et al. (2015) ⁵⁵	Waelz	Pressurized Batch Reactor	Wet/Slurry Carbonation

Table 2: Summary of process conditions and their general enhancement effects on carbonation conversion extent (indicated by the slope of arrows) of several slag carbonation studies.




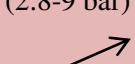



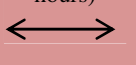
Reference	Slag Type	Temperature	Reaction time	CO ₂ Pressure	L/S ratio	Slurry volume	Particle size	Steam addition	Stirring rate	CO ₂ Flow Rate	Highest CO ₂ conversion (%) achieved
Huijgen et al. (2009) ⁴¹	BOF	(between 25 °C - 200 °C) ↑ (for T >200 °C) ↓	↑	(0-9 bar) ↑ (>9 bar) No clear effect	Highest conversion presented: L/S=2kg/kg. For values lower or higher the conversion extent gets lower	—	↓	—	(0 - 500rpm) ↑ (500-1500rpm) ↔ (1500-2000rpm) ↑	—	74 % (after 30 min, particle size=38µm, T=100 °C, P _{CO2} =19 bar, 500 rpm, and L/S= 10kg / kg)
Chang et al. (2011a) ⁴²	BOF	(30 °C- 60 °C) ↑ (60 °C - 80 °C) ↓	(for the first 60 minutes) ↑ (60min-240min) ↔	Steady (1.013 bar)	Steady (10 mL/g)	—	Steady (< 44 µm)	—	—	↓	68 % (after 60 min, T=70 °C, particle size <44µm, P _{CO2} = 1.013 bar, L/S= 10 mL/g, flow rate=0.1 L/min)
van Zomeren (2011) ⁴⁵	BOF	(L/S: 2 L/kg) (up to 90 °C) ↑ (L/S: 0.1 L/kg) ↔	↑	—	↑	—	Steady (2-3.3 mm)	—	—	Steady (400mL /min)	4.7% (after ~60 hours, T=90 °C, particle size: 2-3.3mm, P _{CO2} =0.2 bar, L/S=2 L/kg, flow rate=0.4 L/min)

Reference	Slag Type	Temperature	Reaction time	CO ₂ Pressure	L/S ratio	Slurry volume	Particle size	Steam addition	Stirring rate	CO ₂ Flow Rate	Highest CO ₂ conversion (%) achieved
Santos et al. (2012) ⁴⁸	BOF (Pressurized Basket Reactor Carbonation)	(more important for lower pCO ₂) ↗	(for 725 °C and 800 °C) Sharp CO ₂ uptake improvement for the initial 7.5 min. (for 575 °C and 600 °C) Gradual uptake improvement with time.	(at 350 °C) ↗ (at 500 °C) Very slight improvement (at 650 °C) ↔	—	—	↖	(more significant in percentage for BOF ₁) ↗ (greater uptakes achieved by BOF ₂)	—	—	~36 % (for BOF ₂ , after 30 min, T=650 °C, particle size <0.08 mm, at total pressure=20 bar)
Chang et al. (2012) ⁴⁴	BOF	(from 25 °C – 65 °C) ↗	(For the first 6 to 7 min) ↗ (10min-30min) ↔	Steady (1 bar)	Steady (20 mL/g)	Steady (1.575 L)	Steady (< 88 μm)	—	(500-1000rpm) ↗ (1000-1250rpm) ↗ ↖	(for the first 15 min and flow rate<1.2m L/min) ↗ (after 15 min) ↔	93.5 % (after 30 min, at T=65°C, particle size=62μm, P _{CO2} =1 bar, L/S=20mL/g, flow rate=1.2 L/min)



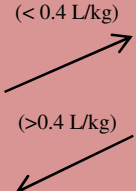







(Table 2 Continued)

Reference	Slag Type	Temperature	Reaction time	CO ₂ Pressure	L/S ratio	Slurry volume	Particle size	Steam addition	Stirring rate	CO ₂ Flow Rate	Highest CO ₂ conversion (%) achieved
Chang et al. (2013) ⁴³	BOF	—	<div> <div>(for the first 10 min)</div> <div>↗</div> <div>(after 10 min)</div> <div>↔</div> </div>	Steady (1.013 bar)	Highest conversion presented: L/S=20mL/g . For values lower or higher than that the conversion extent gets lower.	<div> <div>(300mL- 350 mL)</div> <div>↗</div> <div>(>350 mL- 450 mL)</div> <div>↘</div> </div>	Steady (<44 μm)	—	—	Highest conversion presented: flow rate=1 L/min . For values less or more than that the conversion extent gets lower.	89.4 % (for CRW/BOF slag system after 2h, at T=25 °C, particle size<44 μm, P _{CO₂} = 1.013 bar, flow rate=1L/min, L/S=20mL/g)
Polettini et al. (2015) ⁴⁶	BOF	↗	—	<div> <div>(for CO₂ conc. of 10% and 40% and especially for total pressures <6 bar)</div> <div>↗</div> <div>(for CO₂ conc.=100% the effect is less significant)</div> </div>	Steady (5 L/kg)	—	Steady (63-100μm)	—	—	—	53.6% (after 4h, at T=100 °C, particle size=63-100 μm ,P _{CO₂} =5 bar, L/S= 5 L/kg, CO ₂ Concentration= 40%)





(Table 2 Continued)

Reference	Slag Type	Temperature	Reaction time	CO ₂ Pressure	L/S ratio	Slurry volume	Particle size	Steam addition	Stirring rate	CO ₂ Flow Rate	Highest CO ₂ conversion (%) achieved
Baciocchi et al. (2015) ⁴⁷	BOF (wet)	Steady (50 °C)		(1-10 bar) 	Steady (0.3L/kg)	—	Steady (<125µm)	—	—	—	~ 20 % (L/S:0.3-0.4L/kg, T=50 °C, PCO ₂ =10bar, CO ₂ conc.=100%)
	BOF (slurry)	Steady (100 °C)		(2.8-9 bar) 	Steady (5L/kg)	—	Steady (<150µm)	—	—	—	~ 40 % (L/S:5 L/kg, T=100°C, PCO ₂ =9bar, CO ₂ conc.=100%)
Tai et al. (2008) ³³	SS	(100 °C – 150 °C)  (150 °C - 200 °C) 	(from 0 -1 hour)  (from 1 – 3 hours) 	Steady (80 bar)	Steady (9 L/kg)	Steady (20 mL)	Ranging between 63 – 90 µm	—	Steady (500 rpm)	—	65 % (after 1h, T=150 °C , particle size between 63 and 90µm P _{CO2} =80 bar, rotating speed of 500 rpm)

(Table 2 Continued)

Reference	Slag Type	Temperature	Reaction time	CO ₂ Pressure	L/S ratio	Slurry volume	Particle size	Steam addition	Stirring rate	CO ₂ Flow Rate	Highest CO ₂ conversion (%) achieved
Baciocchi et al. (2009) ⁴⁹	SS			No clear Effect		—		—	—	—	27.15 % (after 8 h, for 40 °C, particle size <0.105mm, P _{CO₂} =3 bar, L/S=0.4 L/kg)
Baciocchi et al. (2010) ³⁸	EAF	Steady (50 °C)		(reaction time < 1 hour) At 1 bar, 30% less CO ₂ uptake than at higher pressures (3 and 10 bar) (reaction time > 1hour) 	Steady (0.4 L/kg)	—		—	—	—	49.1 % (after 24h, T=50 °C, part. size<150 μm, P _{CO₂} =0.3 bar, L/S=0.4 L/kg,)
	AOD	Steady (50 °C)			Steady (0.4 L/kg)	—		—	—	—	69.9 % (after 24h T=50 °C, P _{CO₂} =10 bar, L/S=0.4 L/kg)

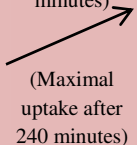
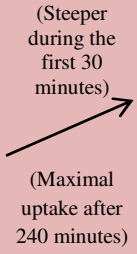
(Table 2 Continued)

Reference	Slag Type	Temperature	Reaction time	CO ₂ Pressure	L/S ratio	Slurry volume	Particle size	Steam addition	Stirring rate	CO ₂ Flow Rate	Highest CO ₂ conversion (%) achieved
Baciocchi et al. (2011) ³⁶	EAF (wet)	Steady (50 °C)		(reaction time < 1 hour) At 1 bar, 30% less CO ₂ uptake than at higher pressures (3 and 10 bar) (reaction time > 1hour) 	Steady (0.4 L/kg)	———	<150 μm	———	———	———	49.1 % (after 24h, T=50 °C , part. size<150 μm, P _{CO₂} =3 bar, L/S=0.4 L/kg,)
	EAF (slurry)	(Until 2 hours and up to 150 °C) 	(P _{CO₂} = 10 bar and T = 100 °C) 	No clear effect	Steady (10 L/kg)	———	<150 μm	———	Steady (500 rpm)	———	38 % (after 4h, T=100 °C , particle size<150μm, P _{CO₂} =10 bar)

(Table 2 Continued)

Reference	Slag Type	Temperature	Reaction time	CO ₂ Pressure	L/S ratio	Slurry volume	Particle size	Steam addition	Stirring rate	CO ₂ Flow Rate	Highest CO ₂ conversion (%) achieved
Vandevelde (2010) ⁵¹	AOD	(carbonation at 30 °C was higher than that at 50 °C) ↙	(steeper during the first 6 hours) ↗ (total duration 7 days)	Steady (1 bar)	(6 hours) (<0.2 L/kg) ↗ (>0.2 L/kg) ↖ (24 hours) (< 0.5 L/kg) ↗	—	—	—	—	—	32% (after 6 days, T=30 °C, L/S=0.2 L/kg, CO ₂ =20%)
	CC	Steady (30 °C)	↗ (total duration 24 hours)	—	—	—	(>25.3 μm) ↖ (<25.3 μm) ↗	—	—	—	45% (after 6 days, T=30 °C, L/S=0.25 L/kg, CO ₂ =20%)

(Table 2 Continued)

Reference	Slag Type	Temperature	Reaction time	CO ₂ Pressure	L/S ratio	Slurry volume	Particle size	Steam addition	Stirring rate	CO ₂ Flow Rate	Highest CO ₂ conversion (%) achieved
Santos et al. (2011) ³⁷	AOD	Steady (50 °C)		————	Steady (1 L/10g)	————	Ranging between 63 and 200 µm	————	Steady (340 rpm)	Steady (0.24 L/min)	30.5% (after 4 hours, T=50 °C, particle size= 60-200µm, L/S=100 , no sonication) 48.5% (under the same conditions, with sonication)
	CC	Steady (50 °C)		————	Steady (1 L/10g)	————	Ranging between 63 and 200 µm	————	Steady (340 rpm)	Steady (0.24 L/min)	61.6% (after 4 hours, T=50 °C, particle size= 60-200µm, L/S=100, no sonication) 73.2% (under the same conditions, with sonication)




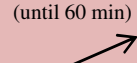







(Table 2 Continued)

Reference	Slag Type	Temperature	Reaction time	CO ₂ Pressure	L/S ratio	Slurry volume	Particle size	Steam addition	Stirring rate	CO ₂ Flow Rate	Highest CO ₂ conversion (%) achieved
Van Bouwel (2012) ⁵³	AOD	<div> <div><60 °C</div> <div> <div></div> <div></div> </div> <div>60 °C-90 °C</div> <div> <div></div> <div></div> </div> <div>90 °C – 180 °C</div> <div> <div></div> <div></div> </div> </div>	<div> <div></div> <div></div> </div> <div> <div></div> <div></div> </div>	<div> <div></div> <div></div> </div> <div> <div></div> <div></div> </div>	<div> <div></div> <div></div> </div> <div> <div></div> <div></div> </div>	<div> <div></div> <div></div> </div> <div> <div></div> <div></div> </div>	Steady (46.1 μm)	—	Steady (1000rpm)	—	63% (after 1 hour, T=90 °C, particle size=46.1 μm, P _{CO2} =30bar and L/S=16)
	CC	<div> <div><60 °C</div> <div> <div></div> <div></div> </div> <div>>60 °C</div> <div> <div></div> <div></div> </div> </div>	<div> <div></div> <div></div> </div> <div> <div></div> <div></div> </div>	<div> <div></div> <div></div> </div> <div> <div></div> <div></div> </div>	<div> <div></div> <div></div> </div> <div> <div></div> <div></div> </div>	<div> <div></div> <div></div> </div> <div> <div></div> <div></div> </div>	Steady (39.3 μm)	—	Steady (1000rpm)	—	76% (after 1 hour, T=90 °C, particle size=39.3μm, P _{CO2} =30bar, L/S ratio=16)

(Table 2 Continued)

Reference	Slag Type	Temperature	Reaction time	CO ₂ Pressure	L/S ratio	Slurry volume	Particle size	Steam addition	Stirring rate	CO ₂ Flow Rate	Highest CO ₂ conversion (%) achieved
Santos et al. (2013) ³⁹	AOD	<p>(from 30 °C – 60 °C)</p> <p>(from 60 °C -90 °C)</p> <p>(from 90 °C -120°C)</p> <p>(>120 °C)</p> <p>(Higher conversion achieved at 120 °C)</p>	(Very sharp increase for the first minute of reaction)	<p>(until 15 bar)</p> <p>(>15 bar)</p> <p>(slight decrease)</p>	<p>(L/S<8L/kg)</p> <p>(slight increase)</p> <p>(L/S>8L/kg)</p>	<p>(for the thin film carbonation experiments)</p> <p>Steady (133.3 mL)</p>	46.1 μm	—	Steady (1000rpm)	—	<p>24.2%</p> <p>(after 144 hours, thin film carbonation, T= 30 °C, particle size=46.1 μm, P_{CO2}=0.2 atm, and L/S=25wt%)</p> <p>44%</p> <p>(after 60mins, slurry carbonation, T=90 °C, particle size=46.1μm P_{CO2}=15 bar, and S/L=62.5g/L)</p>
	CC	<p>(from 30 °C-90 °C)</p> <p>(from 90 °C-120°C)</p> <p>(>120 °C)</p> <p>(Higher conversion achieved at 90 °C)</p>	(Very sharp increase for the first minute of reaction)	<p>(until 9 bar)</p> <p>(9 bar-12 bar)</p> <p>(>12 bar)</p>	<p>(L/S<16L/kg)</p> <p>(L/S>16L/kg)</p>	<p>(for the slurry set of experiments)</p> <p>Ranging between 820 mL and 1L</p>	39.3 μm	—	Steady (1000rpm)	—	<p>37%</p> <p>(after 144 hours, T=30 °C. particle size=39.3μm, P_{CO2}=0.2atm, and L/S= 25wt%)</p> <p>57%</p> <p>(after 60 mins, slurry carbonation at T=90 °C, particle size=39.3 μm P_{CO2}=30 bar, and S/L=60g/L)</p>

(Table 2 Continued)

Reference	Slag Type	Temperature	Reaction time	CO ₂ Pressure	L/S ratio	Slurry volume	Particle size	Steam addition	Stirring rate	CO ₂ Flow Rate	Highest CO ₂ conversion (%) achieved
Chang et al. (2011b) ⁴⁰	BF	(for P _{CO₂} =48.3 bar, from 40 °C – 100°C)  (for P _{CO₂} =48.3bar, from 100 °C – 160 °C)  (for P _{CO₂} =89.6bar, from 40 °C – 160 °C) 	(until 60 min)  (after 60 min) 	Conversion under 89.6 bar was slightly lower than the conversion under 48.3 bar	(Until 10 mL/g)  (10-20 mL/g)  (>20 mL/g) 	—	Steady (<44 μm)	—	—	—	68.3 % (after 12 h, at T=160 °C, particle size<44μm, P _{CO₂} =48 bar L/S ratio=10mL/g)
Cappai et al. (2015) ⁵⁵	Waelz slag	Steady (25 °C)		(after 24 h of reaction) 		—	Steady (<4 mm)	—	—	—	18.3 % (after 240h, at T=25 °C, particle size < 4 mm, P _{CO₂} =20 bar, L/S ratio=1mL/g)

(Table 2 Continued)



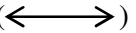

Legend: **BF** is the Blast Furnace slag, **BOF** is the Basic Oxygen Furnace slag, **EAF** is the Electric Arc Furnace slag, **AOD** is the Argon Oxygen Decarburization slag, **CC** is the Continuous Casting slag, and **SS** is the Stainless Steel slag, which most of the times is a mixture of EAF and AOD slag provided by stainless steel manufacturing industries. The arrows indicate **increase** () or **decrease** () of the carbonation extent **in relation to the increase** (unless otherwise stated) of the **examined parameter**. This symbol () is used when **no alteration** of the carbonation extent is observed with increasing of the examined parameter's value. Whenever no clear effect of the alterations of the parameters is observed in the carbonation extent, it is clearly mentioned **“No clear effect”**. When the effect of a parameter is not tested in an experiment or there is no information about this parameter, this symbol () is used.

Table 3: Summary of slag and process parameters from different carbonation studies and the resulting calculated Carbonation Weathering Rate (CWR).

	Type of Slag	Particle diameter (μm)	$r_x(\mu\text{m})$	Conversion, C% (%)	$t_{carb}(\mu\text{m})$	Reaction time, $\tau_{\text{react}}(\text{min})$	CWR ($\mu\text{m}/\text{min}$)
Huijgen et al. (2009) ⁴¹	BOF	38	19	74	6.87	30	0.229
Chang et al. (2011a.) ⁴²	BOF	44	22	68	6.95	60	0.116
Van Zomeren (2012) ⁴⁵	BOF	2000-3300	1000-1650	4.67	16.95 – 27.97	3600	0.004 – 0.007
Santos et al. (2012) ⁴⁸	BOF	80	40	36	5.53	30	0.184
Chang et al. (2012) ⁴⁴	BOF	62	31	93.5	18.54	30	0.618
Chang et al. (2013) ⁴³	BOF	44	22	89.4	11.59	120	0.097
Polettini et al. (2015) ⁴⁶	BOF	63-100	31.5-50	53.6	7.11 – 11.29	240	0.030 – 0.047
Baclocchi et al. (2015) ⁴⁷	BOF(wet)	125	62.5	20	4.48	1440	0.003
	BOF(slurry)	150	75	40	11.74	1440	0.008
Tai et al. (2008) ³³	SS	63-90	31.5-45	65	9.30 – 13.29	60	0.155 – 0.221
Baclocchi et al. (2009) ⁴⁹	SS	105	52.5	27.2	5.26	480	0.011
Baclocchi et al. (2011) ³⁶	EAF(wet)	150	75	34.3	9.80	1440	0.007
	EAF(slurry)	150	75	25.4	7.00	240	0.029
Baclocchi et al. (2010) ³⁸	AOD	150	75	69.9	50.73	1440	0.017
Vandeveld (2010) ⁵¹	AOD	38.7	19.35	32	2.33	8640	0.00027
	CC	40.7	20.35	45	3.67	8640	0.00043

Santos et al. (2011) ³⁷	AOD(mechanical)	60-230	30-115	30.5	3.43 – 13.14	240	0.0143 – 0.0547
	CC(mechanical)	60-230	30-115	61.6	8.20 – 31.41	240	0.0341 – 0.1309
	AOD(sonication)	60-230	30-115	48.5	5.95 – 22.82	240	0.025 – 0.095
	CC(sonication)	60-230	30-115	73.2	10.66 – 40.86	240	0.044 – 0.170
Van Bouwel (2012) ⁵³	AOD	46,1	23.05	63	6.50	60	0.108
	CC	39.3	19.65	76	7.44	60	0.124
Santos et al. (2013) ³⁹	AOD(wet)	46.1	23.05	24.2	2.03	8640	0.000235
	CC(wet)	39.3	19.65	37	2.81	8640	0.000325
Santos et al. (2013) ³⁹	AOD(slurry)	46.1	23.05	44	4.05	60	0.068
	CC(slurry)	39.3	19.65	57	4.82	60	0.080
Chang et al. (2011b.) ⁴⁰	BF	44	22	68.3	7.00	720	0.010
Cappai et al. (2015) ⁵⁵	Waelz	4000	2000	18.3	130.46	14400	0.009

(Table 3 Continued)

Influence of process parameters on carbonation rate and conversion of steelmaking slags – Introduction of the ‘carbonation weathering rate’

Georgakopoulos, Evangelos

2016-07-05

Attribution-NonCommercial 4.0 International

Georgakopoulos, E. et al. (2016) Influence of process parameters on carbonation rate and conversion of steelmaking slags – Introduction of the ‘carbonation weathering rate’, Greenhouse Gases: Science and Technology, Vol. 6, Iss. 4, pp. 470-491

<http://dx.doi.org/10.1002/ghg.1608>

Downloaded from CERES Research Repository, Cranfield University